1   **Plants face the flow in V-formation: a study of plant patch alignment in streams**

2   Authors:

3   Loreta Cornacchia[1,7, a]   loreta.cornacchia@nioz.nl, loreta.cornacchia@univ-lyon1.fr
4   Andrew Folkard[2]   a.folkard@lancaster.ac.uk
5   Grieg Davies[3]   grieg.davies@southernwater.co.uk
6   Robert C. Grabowski[4]   r.c.grabowski@cranfield.ac.uk
7   Johan van de Koppel[1,7]   johan.van.de.koppel@nioz.nl
8   Daphne van der Wal[1,8]   daphne.van.der.wal@nioz.nl
9   Geraldene Wharton[5]   g.wharton@qmul.ac.uk
10   Sara Puijalon[6]   sara.puijalon@univ-lyon1.fr
11   Tjeerd J. Bouma[1,7]   tjeerd.bouma@nioz.nl
12
13   Affiliations:

14   [1] NIOZ Royal Netherlands Institute for Sea Research, Department of Estuarine and Delta
15   Systems, and Utrecht University, P.O. Box 140, 4400 AC Yerseke, the Netherlands.

16   [2] Lancaster Environment Centre, Lancaster University, Lancaster, UK

17   [3] Southern Water Services, Southern House, Worthing, UK

18   [4] Cranfield Water Science Institute, Cranfield University, Cranfield, UK

19   [5] School of Geography, Queen Mary University of London, London, UK

20   [6] Univ Lyon, Université Claude Bernard Lyon 1, CNRS, ENTPE, UMR 5023 LEHNA, F-69622,
21   Villeurbanne, France

22   [7] Groningen Institute for Evolutionary Life Sciences, University of Groningen, PO Box 11103,
23   9700 CC Groningen, The Netherlands

24   [8] Faculty of Geo-Information Science and Earth Observation (ITC), University of Twente, P.O.
25   Box 217, 7500 AE Enschede, The Netherlands

26   [a] Present address: UMR 5023 LEHNA, Université Lyon 1, CNRS, ENTPE, Villeurbanne Cedex,
27   France

28   Corresponding author:
29   Loreta Cornacchia
30   NIOZ Royal Netherlands Institute for Sea Research
31   Korringaweg 7
32   4401 NT Yerseke
33   The Netherlands
34   email: loreta.cornacchia@nioz.nl
35   Tel.:   +31 (0)113 577 457
36   Fax: +31 (0)113 573 616
37

Abstract

42   Interactions between biological and physical processes, so-called bio-physical feedbacks, are

43   important for landscape evolution. While these feedbacks have been quantified for isolated patches

44   of vegetation in aquatic ecosystems, we still lack knowledge of how the location of one patch

45   affects the occurrence of others. To test for patterns in the spatial distribution of vegetation patches

46   in streams, we first measured the distance between *Callitriche platycarpa* patches using aerial

47   images. Then, we measured the effects of varying patch separation distance on flow velocity,

48   turbulence, and drag on plants in a field manipulation experiment. Lastly, we investigated whether

49   these patterns of patch alignment developed over time following locations of reduced

50   hydrodynamic forces, using two-year field observations of the temporal patch dynamics of

51   *Ranunculus penicillatus* in a lowland chalk stream. Our results suggest that vegetation patches in

52   streams organize themselves in V-like shapes to reduce drag forces, creating an optimal

53   configuration that decreases hydrodynamic forces and may therefore encourage patch growth.

54   Downstream patches are more frequently found at the rear and slightly overlapping the upstream

55   patch, in locations that are partially sheltered by the established upstream vegetation while ensuring

56   exposure to incoming flow (important for nutrient availability). Observations of macrophyte patch

57   dynamics over time indicated that neighbouring patches tend to grow in a slightly angled line,

58   producing a spatial pattern resembling the V-formation in migratory birds. These findings point to

59   the general role of bio-physical interactions in shaping how organisms align themselves spatially to

60   aero- and hydrodynamic flows at a range of scales.

Introduction

Biogeomorphic landscapes, such as rivers, mangroves and salt marshes, are characterized by strong interactions between biological and physical processes. These reciprocal interactions, also referred to as bio-physical feedbacks, are fundamental for landscape formation, adjustment, and evolution (Corenblit et al. 2007; Murray et al. 2008; Corenblit et al. 2015). By obstructing the flow, vegetation stimulates channel formation in tidal marsh landscapes (Temmerman et al. 2007; Kearney and Fagherazzi 2016). In fluvial environments, riparian and floodplain plants affect the processes and morphology of alluvial rivers (Tal and Paola 2007; Gurnell 2014). Such environments are characterized by the presence of ecosystem engineers (Jones et al. 1994; Gurnell 2014), organisms that are able to modify their habitat through their action or their own physical structure or actions. To understand these biogeomorphic systems, many studies have focused on interactions between vegetation, hydrodynamics, and sedimentation processes (Leonard and Luther 1995; Madsen et al. 2001; Bouma et al. 2007). These landscapes are often characterised by patchy vegetation, at least during the establishment phase. However, despite many plants being the keystone species in these environments, understanding of how flow modification at the patch scale may affect the processes and mechanisms controlling vegetation establishment and the hydrodynamics of these systems remains limited.

The interactions between flowing water and plants have been studied across different ecosystems, over a variety of spatial scales and vegetation configurations. Such configurations include homogeneous fields of vegetation (Kouwen and Unny 1973; Nepf and Vivoni 2000; Chen et al. 2013) as well as isolated plant patches (Sand-Jensen and Vindbœk Madsen 1992; Bouma et al. 2009; Zong and Nepf 2012). The impact of a vegetation patch on hydrodynamics and sediment dynamics is location and scale-dependent (Rietkerk and Van de Koppel 2008; van Wesenbeeck et

84   al. 2008; Schoelynck et al. 2012), for instance changing from reduced flow velocities within the

85   vegetation to increased velocities around it. Many more studies have been carried out on individual

86   patches of submerged aquatic macrophytes (for example, Sand-Jensen and Mebus, 1996; Sand-

87   Jensen, 1998; Sukhodolov and Sukhodolova, 2009), compared to studies with multiple macrophyte

88   stands (Cotton et al. 2006; Wharton et al. 2006; Marjoribanks et al. 2017). As patches in a

89   landscape rarely grow in isolation but rather in mosaics (Temmerman et al. 2007; Van der Wal et al.

90   2008), including a pseudo-braided pattern in rivers (Dawson 1989), one patch may affect other

91   patches by altering its local environment. The size of the gap between vegetation patches can be

92   influenced by current velocity (Fonseca and Bell 1998) and turbulence, and has implications for

93   physical and ecological processes (e.g. sedimentation, nutrient availability) (Folkard 2005; Folkard

94   2011). Recent attention has been focused on the larger-scale impact of multiple patches, and how

95   their size and/or alignment affects flow patterns (Folkard 2005; Vandenbruwaene et al. 2011;

96   Adhitya et al. 2014) and sediment deposition (Meire et al. 2014), and the implications for landscape

97   adjustments and evolution (Kondziolka and Nepf 2014; De Lima et al. 2015; Gurnell and

98   Grabowski 2016). However, knowledge is still lacking on how the location of one patch may affect

99   the occurrence of another patch, potentially leading to optimal spatial configurations due to

100   hydrodynamic force reduction.

101   Several studies have revealed the importance of facilitation, i.e. positive interactions

102   between species that promote establishment by mediation of physical stress (Bruno et al. 2003;

103   Callaway 2007). Thus, positive feedbacks created by one patch may extend beyond the patch itself

104   (Bruno and Kennedy 2000), leading to a facilitative effect on the establishment or growth of other

105   species. Such interactions between vegetation patches are likely to be relevant for plant

106   establishment in lotic environments, where primary colonization is challenging due to forces that

4

107 act to dislodge seedlings and fragments (Riis 2008; Balke et al. 2014). However, studies of

108 facilitation mostly focus on interactions between individuals of different species or interspecific

109 interactions (Bruno et al. 2003; Callaway 2007). Consequently, we know relatively little about

110 intraspecific facilitation mediated by existing vegetation patches of the same species and its effects

111 on distribution patterns in the landscape. It is important to address this gap as intraspecific

112 facilitation is likely to be a key process in flow-dominated systems, where currents and drag forces

113 may impose a stress that limits growth and seedling establishment (Schutten et al. 2005; Puijalon et

114 al. 2008; Balke et al. 2011). It is known that vegetation patches may increase flow velocity in some

115 adjacent areas, while reducing it directly downstream of the patch (Bouma et al. 2007; Chen et al.

116 2012; Schoelynck et al. 2012). As a consequence, optimal spatial configurations of vegetation

117 patches might be expected to emerge due to patterns of hydrodynamic force reduction, specifically

118 in terms of drag force reduction.

119   Plant-flow interactions have been studied intensively in vegetated streams because of their

120 ecological and geomorphological importance (Gurnell 2014; Bertoldi et al. 2015; Grabowski and

121 Gurnell 2016), and the presence of unidirectional flow makes them an ideal model system. In this

122 study, we investigated the spatial distribution of submerged aquatic vegetation patches and the

123 implications of this for in-stream landscape adjustments over a two-year timescale. There were

124 three components to the study. First, naturally occurring macrophyte patches were identified from

125 aerial images to determine the average patch separation distances. Then, a field manipulation

126 experiment was conducted to measure the effects of varying patch separation distance on flow

127 velocity, turbulence, and drag on the submerged plants. We considered drag reduction as a proxy

128 for the benefits derived by plants from their location in relation to other patches. Previous studies

129 indicate that, on a short temporal scale, the survival and establishment of individual plants depend

130   on successful root development (in the order of days; Barrat-Segretain et al. (1998); Barrat-

131   Segretain et al. (1999)) and protection from scouring or dislodgement due to currents and drag.

132   Most of this primary colonization phase derives from drifting vegetative fragments, and rarely from

133   seeds (Sand-Jensen et al. 1999; Riis 2008). To test whether the most frequent patch distributions

134   corresponded to the locations with the lowest drag forces, we related patterns of drag reduction to

135   the observed probability of patch occurrence identified from aerial images. After colonization,

136   single shoots develop into patches on intra-annual time scales through clonal expansion (over the

137   course of months; Cotton et al. (2006); Wharton et al. (2006)). Therefore, finally we tested whether

138   such preferential patch distributions obtained from aerial images were supported by field

139   observations of temporal patch dynamics in a lowland chalk stream over a period of two years.

140   Materials and methods

141   Measuring inter-patch distance from in-stream aerial images

142   To investigate the existence of preferential distributions of plant patches, we collected aerial images

143   of an artificial drainage channel with natural colonization by aquatic vegetation. The channel is

144   located along the Rhône River (France), near Serrières-de-Briord (45.8153 ° N, 5.4274 ° E). The

145   channel, selected for its uniform cross-sectional and planform geometry allowing a focus on plant

146   configuration, had an average channel width of 8.0 m, an average depth of 0.8 m, rarely exceeding

147   1.3 m, with relatively straight banks. Aerial images of the streambed were taken with a digital

148   camera mounted on a pole at a height of c. 2 m. We identified 22 pairs of neighbouring patches for

149   the dominant aquatic macrophyte *Callitriche platycarpa*. This species has long, flexible shoots that

150   are pushed in a downstream direction by the flow, generating an overhanging canopy that is rooted

151   only at the upstream edge (Haslam 1978). The pairs could clearly be distinguished as separate

152   patches through the presence of an unvegetated area between their rooting parts. In these streams,

153   neighbouring patches were defined as those within 1.5 m from each other, because the influence of

154   an upstream patch can be observed for a distance equal to its length (Sand-Jensen and Mebus 1996;

155   Schoelynck et al. 2012), and 1.5 m is representative of the average length of *C. platycarpa* patches

156   (Sand-Jensen 1998). We measured the absolute longitudinal inter-patch distance (distance between

157   their upstream edges in the streamwise direction, L_d in m) and transversal inter-patch distance

158   (distance between their leftmost edges in the spanwise direction, T_d in m) between the pairs (Figure

159   1). To account for differences in absolute distances due to the variability in patch sizes, we

160   converted them into relative distances. To obtain relative longitudinal distances (L), we divided the

161   absolute distance L_d by the length of the upstream patch L_u. To obtain relative transversal distances

162   (T), we divided the absolute distance T_d by the width of the upstream patch T_u (Figure 1). The

163   frequency distributions of relative longitudinal and transversal distances were first converted into

164   probability distributions. Then, the probability distributions in the two directions were multiplied by

165   each other to obtain the probability of naturally-observed occurrences of vegetation patches for

166   each combination of L and T distances. This point grid was imported into GIS software and

167   interpolated to obtain a two-dimensional probability map of naturally-observed patch occurrence

168   (%) at different distances from an existing patch, using kriging interpolation.

169   **Quantifying the effects of inter-patch distance on flow velocity and drag using a field**

170   **manipulation experiment**

171   *Flow velocity measurements*

172   To assess the effects of different patch configurations on flow reduction and acceleration, we

173   measured the changes in flow velocity with varying patch separation distance through a field

174   manipulation. Plants were detached from existing patches, transplanted on perforated metal plates

175   and fixed through cable ties at the roots, to recreate two *C. platycarpa* patches (1.2 m in length, 0.6

176   m in width) that could be moved and arranged at different distances in the river bed. The two

177   patches were arranged into 10 different configurations, representing a combination of longitudinal

178   and transversal distances (Figure 2). The patch located upstream ("patch U") was kept fixed, while

179   the other one ("patch D") was moved downstream and/or laterally to create the configurations. The

180   two patches were partially overlapping in one configuration (T = 0.5, L = 0.46), as the leading edge

181   of patch D started at the end of the rooted area of patch U. In this case, the overhanging canopy of

182   patch U was located in the upper water layer, while the leading edge of patch D was located close

183   to the bed, which still allowed water to flow in between the two patches. The patch characteristics

184   (width, length and density) were kept constant between the fixed and mobile patches. Patch density

185   was fixed by fitting the plants into the perforated metal plates, with an array of 9408 holes per m^2.

186   The condition of the plant patches did not deteriorate during the course of the experiment, thus

187   maintaining a similar morphological function within the river.

188   Vertical profiles of flow velocity were measured with a 3D acoustic Doppler velocimeter

189   (ADV, Nortek) over 2 min at 10 Hz. Hydrodynamic profiles were measured at five vertical

190   locations of 5, 10, 20, 40 and 90% of the depth above the river bed. Around the pair of vegetation

191   patches, vertical profiles were located at distances of 0.2 m and 0.1 m respectively from the

192   upstream edges, and 0.2 m on both sides of each patch (at 0.35 m along their length), i.e. in the gap

193   between the patches. For each point measurement in the profile, mean values of the velocity

194   components *u, v* and *w* were calculated (corresponding to velocities in the *x, y* and *z* directions; m s⁻

195   ¹). Depth-averaged flow velocities *u* (in the streamwise direction) are expressed relative to

196   incoming flow velocity, which was recorded at a fixed measurement point located 0.5 m upstream

197   of patch U.

Turbulent kinetic energy

199   To determine the effects of different patch configurations on turbulence, we measured the changes

200   in turbulent kinetic energy (TKE, $m^2\ s^{-2}$) with different patch separation distances. TKE is a

201   measure of hydrodynamic turbulence that can negatively affect plants through direct effects on their

202   growth (Jaffe and Forbes 1993). Also, by governing processes of sediment trapping and

203   resuspension (Hendriks et al. 2008), it can potentially affect plant establishment by reducing

204   sediment stability. TKE was therefore calculated for the profile located at 0.1 m from the upstream

205   edge of patch D, to investigate its potential implications for establishment. We first calculated the

206   turbulent fluctuations $u'(t) = u(t) - \overline{u}$ where $u(t)$ is the time series of flow measurements and $\overline{u}$

207   is the time-averaged velocity ($m\ s^{-1}$) in the streamwise direction at each vertical position. The

208   corresponding spanwise and vertical turbulent velocity components v' and w' were calculated in

209   the same way. For each point measurement in the profile, turbulent kinetic energy (per unit mass)

210   was then calculated as $TKE = \frac{1}{2}\left(\overline{u'^2} + \overline{v'^2} + \overline{w'^2}\right)$.

Drag force measurements

212   To investigate the benefits of different patch configurations in terms of drag reduction, we

213   measured the effects of varying patch separation distance on drag forces. Drag forces were

214   measured using a force transducer developed by the former WL Delft Hydraulics (now Deltares,

215   Delft, The Netherlands). The transducer consisted of a solid platform, carried by two steel

216   cantilever beams, with four temperature-corrected strain gauges mounted in pairs on opposite sides

217   of each of the two steel cantilevers (for details see Bouma et al. (2005)). The voltage output for the

218   force transducer was linearly correlated with forces up to 10 N ($r^2 = 0.99$, p < 0.001). During the

219   measurements, a *C. platycarpa* plant was mounted on top of the transducer and placed into the river

220   bed at the upstream edge of patch D. For the measurements, we selected isolated plants of 55.1 ±

221   5.8 cm in height and with 4 to 9 ramifications. Plants were attached to the transducer by their stem,

222   and positioned in a natural growth position to closely represent the natural conditions. Voltage

223   readings were collected on a data logger at a frequency of 100 Hz and expressed as the mean value

224   for 1 min. As bending and leaning of the plant on the vegetation patch interferes with measuring the

225   actual drag on the individual, drag measurements were also performed by removing patch D and

226   repeating the measurement on the single plant. To allow comparisons between individuals, drag

227   was expressed as a function of total plant surface area.

228   **Effects of patch interactions on seasonal in-stream landscape adjustments: evidence from**

229   **temporal field surveys**

230   To test whether new vegetation occurred preferentially at certain distances and directions from

231   initial vegetation patches, we analysed field surveys of vegetation development from a study on a

232   chalk stream reach within the Frome-Piddle catchment (Dorset, UK) over two years (monthly from

233   July 2008 to July 2009, and bimonthly thereafter until July 2010; for further information on the

234   field surveys, please see Davies (2012)). The study reach was the Bere Stream (UK Grid Reference

235   385563, 93009), a relatively straight 30 m section with bankfull widths ranging between 7-9 m. The

236   dominant in-channel aquatic macrophyte was water crowfoot (*Ranunculus penicillatus* subsp.

237   *pseudofluitans*) which has highly similar patch establishment dynamics and structural traits to

238   *Callitriche platycarpa* (rooted at the upstream part of the patch and with very flexible stems that

239   form an overhanging canopy; Haslam 1978). Furthermore, the main factors affecting initial

10

240   establishment are determined by mechanical forces (e.g. drag, flow velocity). These forces increase

241   the risk of plant uprooting or dislodgement and relate to plant morphological characteristics (Bal et

242   al. 2011), rather than species characteristics such as growth rates. Thus, field observations of

243   *Ranunculus* could be compared with the findings of the field manipulation experiments of *C.*

244   *platycarpa*.

245   The data set from the Frome-Piddle catchment afforded a unique opportunity to assess the

246   occurrence of new vegetation and changes in vegetation cover and spatial distribution over time.

247   The field survey was a repeated measures design over time. During each survey, macrophyte

248   distribution was mapped along 30 transects that were located at 1-m distance intervals along the 30-

249   m long study reach. Along each transect, measurement points were located at 0.5 m intervals to

250   record macrophyte presence and species. The sample size was 2150 measurement points, replicated

251   over 19 surveys, of which six surveys were used in this study. Reach survey data were analysed

252   using GIS software. The total station coordinates of the transect markers were used to georeference

253   a digitised version of the reach within a GIS. The output resulted in an array of points that were

254   spatially arranged along transect lines. Vegetation cover observed at points in the reach data set

255   were interpolated using an Inverse Distance Weighted (IDW) interpolation method. If the predicted

256   surface outputs from IDW differed from the substrate cover observed at any extra observation point

257   not used in the IDW, the substrate cover observed at that point prevailed above the IDW

258   interpolation. Separate vegetation patches were derived using the minimum bounding geometry

259   enclosing each of the polygon outputs from IDW. Although not measured in this study, seasonal

260   changes in macrophyte cover are generally associated with changes in vegetation biomass density

261   (g dry weight m^{-2}). A previous study in the Bere Stream found that *Ranunculus* density was lowest

262   during winter (January, about 100 g DW m^{-2}) and peaked during the summer months (May – July),

263   when it reached about 400 g DW m^{-2} (Dawson 1976).

264   We tested the hypothesis that directions of growth of new patches compared to existing

265   patches during the survey period show preferential directions for plant growth, instead of being

266   uniformly distributed in all directions. Therefore, six replicate surveys over three different periods

267   were selected over the two years (December 2008 – July 2009, September 2009 – January 2010,

268   January 2010 – July 2010) because a net increase in *Ranunculus* cover was measured within each

269   of them, allowing the phase of new macrophyte patch colonization to be captured. The shortest

270   distance and direction (angle) between each new vegetation patch and the closest existing patch at

271   the beginning of each survey period were calculated using the 'Near' tool in ArcMap 10.4.

272 **Statistical analyses**

273 In the aerial photography, 22 replicate pairs of patches were considered. A chi-squared test was

274 used to test for significant differences in the frequency of observed longitudinal and transversal

275 distances between vegetation patches. In the field experiment, the statistical design was a fully

276 factorial design with transversal and longitudinal distances as the main factors, comprising ten

277 different configurations (treatments) each measured once. Regression analysis was used to test the

278 effects of varying longitudinal and transversal distances on depth-averaged and near-bed (5 and

279 10% of depth above the river bed) flow velocities in four different positions (between the patches,

280 at the upstream edge of patch D, next to patch U, next to patch D), and on turbulent kinetic energy

281 at the upstream edge of patch D. We tested whether relative flow velocities would increase linearly

282 with increasing inter-patch distances, or follow a quadratic relationship which might be expected if

283 relative flow velocities first increase until a maximum at intermediate distances, and then decrease

284 to 1 as they become equal to incoming flow velocity. In the latter case, patches become far enough

285 apart so that they cease to interact. Hence, we fitted both linear and quadratic models using single

286 (L or T distances) and multiple (L and T distances) predictor variables. We then used Akaike's

287   Information Criterion to compare the adequacy of the candidate models, and selected the model

288   with the lowest AIC score (Akaike 1998). Regression analysis was used to test for the relationship

289   between flow velocities and drag forces on *C. platycarpa* in the field flume experiment. Ordinary

290   Least Square (OLS) regression was used for spatial regression between the experimental drag

291   measured around a vegetation patch, and the probability of naturally-observed patch occurrence.

292   The latter was first log-transformed (natural log of original value + 0.5) due to its skewed

293   distribution. A chi-squared test was used to test for significant differences in angle of growth

294   compared to a uniform distribution in all directions. A paired t-test was used to compare drag forces

295   measured on single plants to drag on plants located at the upstream edge of a vegetation patch.

Results

Observed inter-patch distances between pairs of macrophytes

298   The analysis of aerial photographs from the Rhône River study reach revealed that naturally-

299   occurring *C. platycarpa* stands display a non-random distribution relative to neighbouring patches

300   (Figure 1). We observed that the leading edge of the downstream patch was most frequently located

301   between one third and halfway along the length of the upstream patch (i.e., L = 0.3 – 0.5) (χ^2_8 =

302   20.54, p = 0.008). This longitudinal separation distance was relatively constant, regardless of the

303   size and shape of the patches we analysed (width/length ratios ranged from 0.25 to 0.83). In the

304   transversal direction, the downstream patch was most frequently located at 80% of the width of the

305   upstream patch from the latter's lateral edge (i.e. T = 0.8), hence partially overlapping with, and

306   sheltered by, the overhanging canopy of the patch ahead (χ^2_6 = 14.90, p = 0.021).

Effects of inter-patch distance on flow velocity and turbulence

307

308   Measurements of the hydrodynamic effects of different patch configurations in the Rhône River

309   study reach showed that depth-averaged flow velocity and turbulence patterns were strongly

310   affected by the distance between patches. In between the patches, flow velocity was strongly

311   reduced when the patches were partly overlapping (i.e. for T = 0.5 and L = 0.46), but it increased

312   when a clear separation developed between patches and flow was constricted. We found a

313   significant linear relationship between flow velocities in between the patches and the relative

314   transversal (T, spanwise) distance between the patches ($F_{1,8}$ = 31.45, r^2 = 0.79, p < 0.001; Figure 3a

315   – c; Table 1). When the patches were close together, with no more than a 5 cm gap (T ≤ 1.08), flow

316   velocities between them were reduced and the pair tended to behave more like a single patch.

317   However, flow velocity accelerated when the gap between the patches, and therefore T, increased.

318   In particular, at T = 1.58, flow velocities between the two patches were higher than incoming

319   velocities due to flow constriction (Figure 3b).

320   We found that turbulence was minimized at intermediate distances along the length of an

321   upstream patch, while it increased both when the patches were next to each other and when one was

322   immediately downstream of the other. Turbulent kinetic energy upstream of the patch was

323   significantly related to relative longitudinal distance L through a quadratic relationship ($F_{2,7}$ =

324   5.719, r^2 = 0.62, p = 0.03), the highest TKE occurred when patches were located next to each other

325   (for L = 0; Figure 3d – f). From L=0, TKE decreased with increased relative longitudinal distance

326   until a minimum at L = 0.66, after which it increased again for L > 0.66 as it entered the high TKE

327   region in the wake of the upstream patch. This minimum TKE at L = 0.66 seems to be the point at

328   which there was an optimal combination of sheltering from the oncoming flow by the upstream

329   patch (which increased with L), and minimization of the high TKE region in the wake of the

14

330   upstream patch (which decreased with L). For the mean flow velocities upstream of patch D, results

331   of single and multiple regression showed no significant relationship with T and L distances (Table

332   1).

333   Areas of weakest flow deflection (i.e. reduced hydrodynamic forces) were found around the

334   upstream patch at intermediate longitudinal distances and, in particular, when the two patches were

335   partly overlapping. However, flow deflection increased both when the patches were next to each

336   other and when one was immediately downstream of the other. A significant non-linear (quadratic)

337   relationship was found between flow velocities next to patch U and both relative transversal (T) and

338   relative longitudinal (L) distances ($F_{4,5} = 7.931$, $r^2 = 0.90$, $p = 0.03$; Figure 3g – i; Table 1). As L

339   increased, flow velocity first decreased for intermediate distances (between 0.16 and 0.58), due to

340   weaker flow redirection around the patch. Then, it increased again to become equal to the incoming

341   flow velocity, following a quadratic relationship. As T increased, and therefore the gap between the

342   patches increased, the flow velocity increased until it was equal to the incoming flow velocity for T

343   ≥ 1.5. However, flow velocities next to patch D showed no significant relationship with relative

344   transversal (T) and longitudinal (L) distances (Table 1).

345   Testing the relationship between patch distance and near-bed flow velocities revealed no

346   significant relationship between patch distances and velocities at 5% of the depth above the river

347   bed (Supporting Information, Table S1). A significant quadratic relationship between flow

348   velocities in between the patches and both relative transversal (T) and relative longitudinal (L)

349   distances was confirmed for flow measurements at 10% of the depth (Supporting Information,

350   Table S2).

351   **Effects of inter-patch distances on drag forces**

352 Existing vegetation patches appeared to create sheltered areas where drag was minimized, and new

353 patches were more likely to occur in these locations. Measurements of the drag force derived from

354 a plant's particular location around an existing vegetation patch revealed a significant relationship

355 between flow velocity and drag force per unit surface area on *C. platycarpa* individuals ($r^2 = 0.92$,

356 $p = 0.0001$; Figure 4a). As our field drag force measurements were in the same order of magnitude

357 as measurements performed on the same species in a laboratory flume (Puijalon et al. 2011), we

358 assert that the field set-up provided comparable and accurate measurements. Drag forces ranged

359 from 0.19 to 4.63 N m^{-2}, due to the flow modification by the vegetation patch, with lowest drag

360 forces right along the lateral edge of the patch, at ≥ 0.55 m from the upstream edge. This distance

361 along the length of the patch corresponded to the end of the rooted area and the start of the floating

362 canopy, with the downstream patch forming an angle of 28° relative to the upstream patch. Plotting

363 the drag in an interpolated spatial grid around a patch shows that the most frequent locations of

364 neighbouring patches based on our field observations correspond to positions with intermediate to

365 low drag forces (Figure 4b and d). Furthermore, the probability of observed patch occurrence in a

366 certain position is inversely related to the observed drag force in that position (ordinary least

367 squares spatial regression, $r^2 = 0.28$, $p < 0.0001$, Figure 4c).

368   Comparison of average drag force measurements on single plants, representing the conditions

369 of initial establishment, compared to plants located at the upstream edge of a well-established patch

370 (n = 10 configurations) showed that *C. platycarpa* individuals experience significantly higher drag

371 when alone (Figure 5; paired t-test, $t_{19} = - 2.28$, $p = 0.03$). This observation shows that drag forces

372 on the upstream plants are mitigated by leaning onto other plants in a patch.

373 **Effects of patch interactions on seasonal in-stream landscape adjustments: evidence from**

374   **temporal field surveys**

375   Field surveys over a two year period in the Frome-Piddle catchment (UK) showed that new

376   vegetation patches occurred at specific orientations from existing vegetation patches ($\chi_5^2 = 9.20$, p =

377   0.1 for Dec. 2008 – July 2009; $\chi_5^2 = 12.80$, p = 0.025 for Sept. 2009 – Jan. 2010; $\chi_5^2 = 10.88$, p =

378   0.053 for Jan. 2010 – July 2010, and $\chi_5^2 = 24.34$, p < 0.001 for all survey periods together; Table 2).

379   Within each of the three time periods we analysed, the most common direction of growth was at

380   angles between 0 and 60° from existing patches (with a peak around 30°), in a downstream

381   direction towards the right bank with a second most common direction at angles between 120 and

382   180°, downstream towards the left bank (Figure 6; Table 2). The most common angles of growth

383   found through field surveys are consistent with the angle of 28° found through field measurements

384   and corresponding to a region where drag forces are the lowest (Figure 4). Overall, these

385   observations support the hypothesis that new patches occur in a slightly angled line with respect to

386   existing well-established patches, in locations with reduced hydrodynamic and drag forces (Figure

387   4).

388   The observed seasonal trends of in-stream vegetation growth and die-back were similar over

389   the two survey years in the Frome-Piddle catchment (Table 2; the corresponding changes in fine

390   sediment deposition within *Ranunculus* patches are reported in Davies, 2012). During both years,

391   *Ranunculus* reached its peak cover in the period May – July and began to decline shortly after (until

392   December), due to the seasonal dieback linked to increasing channel discharge and decreasing

393   daylengths and water temperatures. In September 2009, a particularly low *Ranunculus* cover was

394   observed (7%), likely related to the increase in autumn discharges. However, in-stream vegetation

395   started to recover from January onwards, when daylengths increased, with new *Ranunculus* patches

396   recolonizing the stream bed.

Discussion

While most studies of bio-geomorphic feedbacks have focused on isolated or already established patches, our study examined the spatial configuration of patches and quantified where plant patches occur in relation to one another. A key finding was that new vegetation patches in streams organize themselves in V-like shapes during the establishment phase to reduce hydrodynamic and drag forces. Field observations showed that patches are more likely to grow at the end of the rooted area of the upstream patch, where its floating canopy starts (i.e., between one third and halfway down the length of an upstream patch), and slightly off to its side (overlapping with part of their width). Measurements in the field revealed that these locations correspond to areas where drag is reduced, due to partial sheltering from high flow velocities and TKE by well-established vegetation patches. Field manipulations supported this hypothesis, showing that mean flow velocity is reduced by partially overlapping with upstream patches in the across-stream direction, and turbulence is minimized when growing halfway down the length of an upstream patch in the main flow direction. Flow deflection around the upstream patch is weakest when a partial V-shape is formed, suggesting that additional secondary patch growth can occur on the other side of the V. These patterns of patch alignment in formation resemble the formation adopted by migratory birds (Portugal et al. 2014), or the drag-reducing queue formations in spiny lobsters (Bill and Herrnkind 1976). This provides evidence of the role that bio-physical interactions have in shaping the way organisms position themselves spatially in landscapes, in both air- and water flow, across a range of scales.

Facilitative interactions within the landscape of a self-organized species

The positive and negative feedbacks underlying the formation of self-organized patterns have been identified for a wide range of ecosystems (Rietkerk et al. 2002; van de Koppel et al. 2005; Larsen et al. 2007). At the scale of a single patch, it is well known that a positive feedback of reduced flow

420   velocities within patches is linked to a negative feedback limiting lateral growth (Bouma et al.

421   2009; Schoelynck et al. 2012). However, while positive feedbacks are generally observed at a small

422   scale within a patch (Rietkerk and Van de Koppel 2008), knowledge of the larger-scale facilitation

423   of seedling or fragment establishment by a self-organized species is limited. Our study provides a

424   first indication of establishment mechanisms operating at this larger, between-patch scale. We show

425   how an existing vegetation patch modifies flow velocities and resulting drag forces in its

426   surroundings thereby leading to positive or negative effects on the occurrence of other patches,

427   operating at a distance. Facilitative interactions within the same self-organized species, and over

428   larger scales, might therefore be an important but overlooked process determining the evolution of

429   spatial patterns over time.

430   The spacing of the vegetation patches resembles the organized spatial configurations

431   observed in other organisms. For instance, migratory birds maximize the upward motion of air from

432   the bird ahead and reduce drag due to air resistance (Lissaman and Shollenberger 1970;

433   Weimerskirch et al. 2001; Portugal et al. 2014), and fish schools adopt different spatial

434   configurations that can lead to reduced energy expenditure (Ashraf et al. 2017). Our temporal

435   observations showed preferential patch occurrence at 0 to 60° angles from existing patches, with a

436   peak around 30°. This angle is consistent with the 28° angle at which drag on the downstream patch

437   was minimized in the field manipulation. However, the regions of minimum drag force did not

438   strictly correspond to the most frequent location of patch occurrence. This discrepancy could be due

439   to the low number of drag measurement points in that location, or to processes occurring during

440   patch development (e.g. erosion of the upstream patch front and downstream displacement of

441   patches (Sand-Jensen and Vindbœk Madsen 1992), nutrient availability, etc.). The observed

442   vegetation patch configurations might involve a balance between stress reduction and nutrient

19

443   availability. For submerged aquatic plants, the position immediately in the wake of another patch

444   could seem equally or even more beneficial in terms of drag reduction. However, the V position

445   might be a hydrodynamic optimum to maximize drag reduction while still ensuring exposure to

446   light and delivery of nutrients by water flow. Flume experiments on nitrogen uptake showed that

447   ammonium uptake rates for *Callitriche* increased when the patch was located at a leading edge,

448   where it was exposed to higher mean velocity (Cornacchia et al. 2018a). Instead, *Callitriche* had

449   very low ammonium uptake rates when it was immediately downstream of another patch and

450   exposed to low mean velocities. This finding suggests that partial, rather than complete, sheltering

451   by established vegetation can allow more nutrients to be delivered to the downstream patch.

452   Similarly, in mussel beds, aggregation at high densities provides the advantage of protection from

453   physical forces, but also increases competition for food (van de Koppel et al. 2005; De Paoli 2017).

454   Therefore, the balance between reducing stress and maintaining resource availability might be an

455   important factor influencing patch distributions in different self-organized systems. Further

456   measurements of hydrodynamics and nutrient uptake, and/or numerical modelling studies are

457   required to investigate the physical explanation for these patterns such as the V formation.

458   The consistency between the neighbouring patch distances observed for *Callitriche*

459   *platycarpa* and *Ranunculus penicillatus* suggest that such V-shaped settlement might be typical for

460   lotic aquatic environments. Thus, it might be a general process for submerged aquatic vegetation in

461   running waters, at least for species with similar morphologies and experiencing comparable drag

462   forces (Bal et al. 2011). However, vegetation distributions can be more complex than the

463   streamlined, V-shaped patterns described here. Moderate flow velocities and uni-directional flows

464   tend to create a streamlined patch distribution, whereas a near-homogeneous plant cover would

465   emerge in streams with sustained periods of low flow velocities (Cornacchia et al. 2018b).

466　Moreover, a model accounting for interactions between neighbouring patches of emergent

467　vegetation found that wake interactions and resulting deposition patterns influence secondary patch

468　growth (De Lima et al. 2015), yielding complex distributions and not necessarily recognizable V-

469　shapes. More complex patterns in vegetation growth have also been observed in a stream with a

470　rich abundance of aquatic plant species (Cameron et al. 2013). Plant traits could also influence the

471　occurrence of recognizable V-shaped patterns. For instance, a V pattern might not be expected for

472　species showing high resistance to hydrodynamic forces (Puijalon et al. 2011), high root anchorage

473　strength (Schutten et al. 2005; Gurnell et al. 2013; Liffen et al. 2013), or relying less on areas of

474　low velocity and fine sediment deposition for their establishment and growth. Our observations

475　were not able to provide evidence of this distribution pattern in other species, which were not as

476　abundant in our field sites. Further studies are necessary to test if a clear dominant species is needed

477　to achieve this configuration, and how the presence of other species might affect the patterns and

478　spacing between patches.

479　　　The patches in our experiment were constructed on an array of 9408 holes per m^2. As a non-

480　dimensional measure of canopy density (Nepf, 2012), *Callitriche* patches have a frontal area per

481　bed area $ah = 0.200 \pm 0.035$ at the incoming flow velocity of 0.24 m s^{-1} (Cornacchia et al. 2018a).

482　This density value is similar to other studies. Bouma et al. (2007) created patches with $ah = 0.64$. In

483　Zong and Nepf (2011), ah ranged from 0.48 to 2.52. These values fall in the dense canopy regime

484　described in Nepf (2012), corresponding to $ah > 0.1$. Therefore, the hydrodynamic patterns

485　presented in this study can generally be expected in other ecosystems with flexible submerged

486　species under dense canopy conditions and presenting similar patch structure (i.e. overhanging

487　canopies).

488　*Initial patterns control future pattern formation: implications for ecosystem resilience*

489 Our results on the role of patchiness on vegetation distribution suggest that initial vegetation

490 patterns determine where future patches occur. This creates patterns at multiple spatial scales: a

491 patch-patch scale during initial establishment, which over time leads to a pseudo-braided pattern in

492 the organization of mature patches at the reach scale, with vegetated bands separated by

493 unvegetated channels. These patterns likely develop on two different time scales. On the scale of

494 generally 1 to 10 days, primary colonization by individual shoots relies on successful root

495 development (Barrat-Segretain et al. (1998); Barrat-Segretain et al. (1999)), which allows them to

496 withstand scouring or dislodgement due to currents and drag (as in our field manipulation). After

497 primary colonization, single shoots develop into patches through clonal growth over the course of

498 months, based on our monitoring data and literature studies (Cotton et al. 2006; Wharton et al.

499 2006). Therefore, the complex self-organized patterning of stream macrophytes likely results from

500 processes interacting at different spatial and temporal scales.

501   Pattern formation at multiple scales, both spatial and temporal, has also been found to

502 increase resilience in mussel beds which are another self-organized ecosystem (Liu et al. 2014).

503 Similar to macrophytes, mussel aggregation into clumps improves their growth and offers

504 protection against hydrodynamic forces (Van de Koppel et al. 2008). Thus, the presence of a few

505 initial patches can facilitate the establishment of new patches. It might promote faster recovery

506 following disturbance events such as floods by creating a self-reinforcing state that increases the

507 resilience of lotic ecosystems. The sheltering effect presumably strengthens as the number of

508 patches increases, eventually developing into near-full vegetation cover (cf. Van der Wal et al.

509 (2008) for *Spartina* tussocks growing into a fully vegetated salt marsh). In regularly disturbed

510 ecosystems, where the hydrologic regime and flow variability are among the primary factors

511 controlling macrophyte establishment and development (Riis and Biggs 2003), this process may be

512 crucially important for vegetation recovery (Barrat-Segretain et al. 1998; Barrat-Segretain et al.

513 1999; Riis 2008). Our study suggests the general role of bio-physical interactions in shaping how

514 organisms align themselves to hydrodynamic flows in different landscapes and across multiple

515 spatial scales.

Acknowledgments

References

525 Adhitya, A., T. Bouma, A. Folkard, M. van Katwijk, D. Callaghan, H. de Iongh, and P. Herman.

526   2014. Comparison of the influence of patch-scale and meadow-scale characteristics on flow

527   within seagrass meadows: a flume study. Marine Ecology Progress Series **516:** 49-59.

528 Akaike, H. 1998. Information theory and an extension of the maximum likelihood principle, p. 199-

529   213. Selected Papers of Hirotugu Akaike. Springer.

530 Ashraf, I., H. Bradshaw, T.-T. Ha, J. Halloy, R. Godoy-Diana, and B. Thiria. 2017. Simple phalanx

531   pattern leads to energy saving in cohesive fish schooling. Proceedings of the National

532   Academy of Sciences **114:** 9599-9604.

533 Bal, K. D., T. J. Bouma, K. Buis, E. Struyf, S. Jonas, H. Backx, and P. Meire. 2011. Trade-off between

534 drag reduction and light interception of macrophytes: comparing five aquatic plants with

535 contrasting morphology. Functional Ecology **25:** 1197-1205.

536 Balke, T., T. J. Bouma, E. M. Horstman, E. L. Webb, P. L. Erftemeijer, and P. M. Herman. 2011.

537 Windows of opportunity: thresholds to mangrove seedling establishment on tidal flats.

538 Marine Ecology Progress Series **440:** 1-9.

539 Balke, T., P. M. Herman, and T. J. Bouma. 2014. Critical transitions in disturbance-driven

540 ecosystems: identifying Windows of Opportunity for recovery. Journal of Ecology **102:** 700-

541 708.

542 Barrat-Segretain, M.-H., G. Bornette, and A. Hering-Vilas-Bôas. 1998. Comparative abilities of

543 vegetative regeneration among aquatic plants growing in disturbed habitats. Aquatic Botany

544 **60:** 201-211.

545 Barrat-Segretain, M.-H., C. P. Henry, and G. Bornette. 1999. Regeneration and colonization of

546 aquatic plant fragments in relation to the disturbance frequency of their habitats. Archiv für

547 Hydrobiologie **145:** 111-127.

548 Bertoldi, W., M. Welber, A. Gurnell, L. Mao, F. Comiti, and M. Tal. 2015. Physical modelling of the

549 combined effect of vegetation and wood on river morphology. Geomorphology **246:** 178-

550 187.

551 Bill, R. G., and W. F. Herrnkind. 1976. Drag reduction by formation movement in spiny lobsters.

552 Science **193:** 1146-1148.

553 Bouma, T., M. De Vries, E. Low, G. Peralta, I. Tánczos, J. van de Koppel, and P. J. Herman. 2005.

554 Trade-offs related to ecosystem engineering: A case study on stiffness of emerging

555 macrophytes. Ecology **86:** 2187-2199.

556 Bouma, T., M. Friedrichs, B. Van Wesenbeeck, S. Temmerman, G. Graf, and P. Herman. 2009.

557   Density-dependent linkage of scale-dependent feedbacks: A flume study on the intertidal

558   macrophyte *Spartina anglica*. Oikos **118:** 260-268.

559 Bouma, T., L. Van Duren, S. Temmerman, T. Claverie, A. Blanco-Garcia, T. Ysebaert, and P. Herman.

560   2007. Spatial flow and sedimentation patterns within patches of epibenthic structures:

561   Combining field, flume and modelling experiments. Continental Shelf Research **27:** 1020-

562   1045.

563 Bruno, J. F., and C. W. Kennedy. 2000. Patch-size dependent habitat modification and facilitation on

564   New England cobble beaches by *Spartina alterniflora*. Oecologia **122:** 98-108.

565 Bruno, J. F., J. J. Stachowicz, and M. D. Bertness. 2003. Inclusion of facilitation into ecological

566   theory. Trends in Ecology & Evolution **18:** 119-125.

567 Callaway, R. M. 2007. Direct Mechanisms for Facilitation, p. 15-116. Positive Interactions and

568   Interdependence in Plant Communities. Springer Netherlands.

569 Cameron, S. M., V. I. Nikora, I. Albayrak, O. Miler, M. Stewart, and F. Siniscalchi. 2013. Interactions

570   between aquatic plants and turbulent flow: a field study using stereoscopic PIV. Journal of

571   Fluid Mechanics **732:** 345-372.

572 Chen, Z., C. Jiang, and H. Nepf. 2013. Flow adjustment at the leading edge of a submerged aquatic

573   canopy. Water Resources Research **49:** 5537-5551.

574 Chen, Z., A. Ortiz, L. Zong, and H. Nepf. 2012. The wake structure behind a porous obstruction and

575   its implications for deposition near a finite patch of emergent vegetation. Water Resources

576   Research **48:** W09517.

577 Corenblit, D., A. Baas, T. Balke, T. Bouma, F. Fromard, V. Garófano-Gómez, E. González, A. M.

578   Gurnell, B. Hortobágyi, and F. Julien. 2015. Engineer pioneer plants respond to and affect

579   geomorphic constraints similarly along water–terrestrial interfaces world-wide. Global

580   Ecology and Biogeography **24:** 1363-1376.

581   Corenblit, D., E. Tabacchi, J. Steiger, and A. M. Gurnell. 2007. Reciprocal interactions and

582   adjustments between fluvial landforms and vegetation dynamics in river corridors: a review

583   of complementary approaches. Earth-Science Reviews **84:** 56-86.

584   Cornacchia, L., S. Licci, H. Nepf, A. Folkard, D. van der Wal, J. van de Koppel, S. Puijalon, and T.

585   Bouma. 2018a. Turbulence-mediated facilitation of resource uptake in patchy stream

586   macrophytes. Limnology and Oceanography**:** doi:10.1002/lno.11070.

587   Cornacchia, L., J. Van De Koppel, D. Van Der Wal, G. Wharton, S. Puijalon, and T. J. Bouma. 2018b.

588   Landscapes of facilitation: how self-organized patchiness of aquatic macrophytes promotes

589   diversity in streams. Ecology **99:** 832-847.

590   Cotton, J., G. Wharton, J. Bass, C. Heppell, and R. Wotton. 2006. The effects of seasonal changes to

591   in-stream vegetation cover on patterns of flow and accumulation of sediment.

592   Geomorphology **77:** 320-334.

593   Davies, G. R. 2012. The transport and retention of fine sediments in seasonally vegetated lowland

594   streams. Queen Mary University of London.

595   Dawson, F. 1976. The annual production of the aquatic macrophyte *Ranunculus penicillatus* var.

596   *calcareus* (RW Butcher) C.D.K. Cook. Aquatic Botany **2:** 51-73.

597   ---. 1989. Ecology and management of water plants in lowland streams. In: Fifty-seventh annual

598   report for the year ended 31st March 1989. Ambleside, UK, Freshwater Biological

599   Association, pp. 43-60. (Annual Report, Freshwater Biological Association, Ambleside).

600   De Lima, P. H., J. G. Janzen, and H. M. Nepf. 2015. Flow patterns around two neighboring patches

601   of emergent vegetation and possible implications for deposition and vegetation growth.

602   Environmental Fluid Mechanics **15:** 881-898.

603   De Paoli, H. 2017. Restoring mussel beds: A guide on how to survive on an intertidal mudflat.

604   University of Groningen.

605   Folkard, A. M. 2005. Hydrodynamics of model *Posidonia oceanica* patches in shallow water.

606   Limnology and Oceanography **50:** 1592-1600.

607   ---. 2011. Flow regimes in gaps within stands of flexible vegetation: laboratory flume simulations.

608   Environmental Fluid Mechanics **11:** 289-306.

609   Fonseca, M. S., and S. S. Bell. 1998. Influence of physical setting on seagrass landscapes near

610   Beaufort, North Carolina, USA. Marine Ecology Progress Series**:** 109-121.

611   Grabowski, R. C., and A. Gurnell. 2016. Hydrogeomorphology—Ecology interactions in river

612   systems. River Research and Applications **32:** 139-141.

613   Gurnell, A. 2014. Plants as river system engineers. Earth Surface Processes and Landforms **39:** 4-25.

614   Gurnell, A., and R. Grabowski. 2016. Vegetation–hydrogeomorphology interactions in a low-energy,

615   human-impacted river. River Research and Applications **32:** 202-215.

616   Gurnell, A. M., M. T. O'Hare, J. M. O'Hare, P. Scarlett, and T. M. Liffen. 2013. The

617   geomorphological context and impact of the linear emergent macrophyte, Sparganium

618   erectum L.: a statistical analysis of observations from British rivers. Earth Surface Processes

619   and Landforms **38:** 1869-1880.

620   Haslam, S. M. 1978. River plants: the macrophyte vegetation of watercourses. Cambridge Univer.

621   Press. Cambridge.

622   Hendriks, I. E., T. Sintes, T. J. Bouma, and C. M. Duarte. 2008. Experimental assessment and

623   modeling evaluation of the effects of the seagrass *Posidonia oceanica* on flow and particle

624   trapping. Marine Ecology Progress Series.

625   Jaffe, M., and S. Forbes. 1993. Thigmomorphogenesis: the effect of mechanical perturbation on

626   plants. Plant Growth Regulation **12:** 313-324.

627 Jones, C. G., J. H. Lawton, and M. Shachak. 1994. Organisms as ecosystem engineers, p. 130-147.
628   Ecosystem management. Springer.

629 Kearney, W. S., and S. Fagherazzi. 2016. Salt marsh vegetation promotes efficient tidal channel
630   networks. Nature Communications **7**.

631 Kondziolka, J. M., and H. M. Nepf. 2014. Vegetation wakes and wake interaction shaping aquatic
632   landscape evolution. Limnology and Oceanography: Fluids and Environments **4:** 106-119.

633 Kouwen, N., and T. E. Unny. 1973. Flexible roughness in open channels. Journal of the Hydraulics
634   Division **99**.

635 Larsen, L. G., J. W. Harvey, and J. P. Crimaldi. 2007. A delicate balance: ecohydrological feedbacks
636   governing landscape morphology in a lotic peatland. Ecological monographs **77:** 591-614.

637 Leonard, L. A., and M. E. Luther. 1995. Flow hydrodynamics in tidal marsh canopies. Limnology
638   and Oceanography **40:** 1474-1484.

639 Liffen, T., A. Gurnell, and M. O'Hare. 2013. Profiling the below ground biomass of an emergent
640   macrophyte using an adapted ingrowth core method. Aquatic botany **110:** 97-102.

641 Lissaman, P., and C. A. Shollenberger. 1970. Formation flight of birds. Science **168:** 1003-1005.

642 Liu, Q.-X., P. M. Herman, W. M. Mooij, J. Huisman, M. Scheffer, H. Olff, and J. Van De Koppel.
643   2014. Pattern formation at multiple spatial scales drives the resilience of mussel bed
644   ecosystems. Nature Communications **5**.

645 Madsen, J. D., P. A. Chambers, W. F. James, E. W. Koch, and D. F. Westlake. 2001. The interaction
646   between water movement, sediment dynamics and submersed macrophytes. Hydrobiologia
647   **444:** 71-84.

648 Marjoribanks, T. I., R. J. Hardy, S. N. Lane, and M. J. Tancock. 2017. Patch-scale representation of
649   vegetation within hydraulic models. Earth Surface Processes and Landforms **42:** 699-710.

650   Meire, D. W., J. M. Kondziolka, and H. M. Nepf. 2014. Interaction between neighboring vegetation

651   patches: Impact on flow and deposition. Water Resources Research **50:** 3809-3825.

652   Murray, A., M. Knaapen, M. Tal, and M. Kirwan. 2008. Biomorphodynamics: Physical-biological

653   feedbacks that shape landscapes. Water Resources Research **44:** W11301.

654   Nepf, H., and E. Vivoni. 2000. Flow structure in depth-limited, vegetated flow. Journal of

655   Geophysical Research: Oceans **105:** 28547-28557.

656   Nepf, H. M. 2012. Flow and transport in regions with aquatic vegetation. Annual Review of Fluid

657   Mechanics **44:** 123-142.

658   Portugal, S. J., T. Y. Hubel, J. Fritz, S. Heese, D. Trobe, B. Voelkl, S. Hailes, A. M. Wilson, and J. R.

659   Usherwood. 2014. Upwash exploitation and downwash avoidance by flap phasing in ibis

660   formation flight. Nature **505:** 399-402.

661   Puijalon, S., T. J. Bouma, C. J. Douady, J. van Groenendael, N. P. Anten, E. Martel, and G. Bornette.

662   2011. Plant resistance to mechanical stress: evidence of an avoidance–tolerance trade-off.

663   New Phytologist **191:** 1141-1149.

664   Puijalon, S., J. P. Léna, N. Rivière, J. Y. Champagne, J. C. Rostan, and G. Bornette. 2008. Phenotypic

665   plasticity in response to mechanical stress: hydrodynamic performance and fitness of four

666   aquatic plant species. New Phytologist **177:** 907-917.

667   Rietkerk, M., M. C. Boerlijst, F. van Langevelde, R. HilleRisLambers, J. v. de Koppel, L. Kumar, H.

668   H. Prins, and A. M. de Roos. 2002. Self-organization of vegetation in arid ecosystems. The

669   American Naturalist **160:** 524-530.

670   Rietkerk, M., and J. Van de Koppel. 2008. Regular pattern formation in real ecosystems. Trends in

671   ecology & evolution **23:** 169-175.

672   Riis, T. 2008. Dispersal and colonisation of plants in lowland streams: success rates and bottlenecks.

673   Hydrobiologia **596:** 341-351.

674   Riis, T., and B. J. Biggs. 2003. Hydrologic and hydraulic control of macrophyte establishment and

675   performance in streams. Limnology and oceanography **48:** 1488-1497.

676   Sand-Jensen, K. 1998. Influence of submerged macrophytes on sediment composition and near-bed

677   flow in lowland streams. Freshwater Biology **39:** 663-679.

678   Sand-Jensen, K., and J. R. Mebus. 1996. Fine-scale patterns of water velocity within macrophyte

679   patches in streams. Oikos **76:** 169-180.

680   Sand-Jensen, K., and T. Vindbœk Madsen. 1992. Patch dynamics of the stream macrophyte,

681   *Callitriche cophocarpa*. Freshwater Biology **27:** 277-282.

682   Sand-Jensen, K., K. Andersen, and T. Andersen. 1999. Dynamic properties of recruitment, expansion

683   and mortality of macrophyte patches in streams. International Review of Hydrobiology **84:**

684   497-508.

685   Schoelynck, J., T. De Groote, K. Bal, W. Vandenbruwaene, P. Meire, and S. Temmerman. 2012. Self-

686   organised patchiness and scale-dependent bio-geomorphic feedbacks in aquatic river

687   vegetation. Ecography **35:** 760-768.

688   Schutten, J., J. Dainty, and A. Davy. 2005. Root anchorage and its significance for submerged plants

689   in shallow lakes. Journal of Ecology **93:** 556-571.

690   Tal, M., and C. Paola. 2007. Dynamic single-thread channels maintained by the interaction of flow

691   and vegetation. Geology **35:** 347-350.

692   Temmerman, S., T. Bouma, J. Van de Koppel, D. Van der Wal, M. De Vries, and P. Herman. 2007.

693   Vegetation causes channel erosion in a tidal landscape. Geology **35:** 631-634.

694   Van de Koppel, J., J. C. Gascoigne, G. Theraulaz, M. Rietkerk, W. M. Mooij, and P. M. Herman.

695   2008. Experimental evidence for spatial self-organization and its emergent effects in mussel

696   bed ecosystems. Science **322:** 739-742.

697 van de Koppel, J., M. Rietkerk, N. Dankers, and P. M. Herman. 2005. Scale-dependent feedback and

698   regular spatial patterns in young mussel beds. The American Naturalist **165:** E66-E77.

699 Van der Wal, D., A. Wielemaker-Van den Dool, and P. M. Herman. 2008. Spatial patterns, rates and

700   mechanisms of saltmarsh cycles (Westerschelde, The Netherlands). Estuarine, Coastal and

701   Shelf Science **76:** 357-368.

702 van Wesenbeeck, B. K., J. Van De Koppel, P. MJ Herman, and T. J Bouma. 2008. Does scale-

703   dependent feedback explain spatial complexity in salt-marsh ecosystems? Oikos **117:** 152-

704   159.

705 Vandenbruwaene, W., S. Temmerman, T. Bouma, P. Klaassen, M. De Vries, D. Callaghan, P. Van

706   Steeg, F. Dekker, L. Van Duren, and E. Martini. 2011. Flow interaction with dynamic

707   vegetation patches: Implications for biogeomorphic evolution of a tidal landscape. Journal

708   of Geophysical Research: Earth Surface **116**.

709 Weimerskirch, H., J. Martin, Y. Clerquin, P. Alexandre, and S. Jiraskova. 2001. Energy saving in

710   flight formation. Nature **413:** 697-698.

711 Wharton, G., J. A. Cotton, R. S. Wotton, J. A. Bass, C. M. Heppell, M. Trimmer, I. A. Sanders, and

712   L. L. Warren. 2006. Macrophytes and suspension-feeding invertebrates modify flows and

713   fine sediments in the Frome and Piddle catchments, Dorset (UK). Journal of Hydrology **330:**

714   171-184.

715 Zong, L., and H. Nepf. 2011. Spatial distribution of deposition within a patch of vegetation. Water

716   Resources Research **47:** W03516.

717 ---. 2012. Vortex development behind a finite porous obstruction in a channel. Journal of Fluid

718   Mechanics **691:** 368-391.

719

720 **Table 1** Regression results of linear and quadratic models including single (T, L) or multiple (T and

721 L) predictor variables. Final selected models (in bold) are based on Akaike Information Criterion

722 (AIC) values.

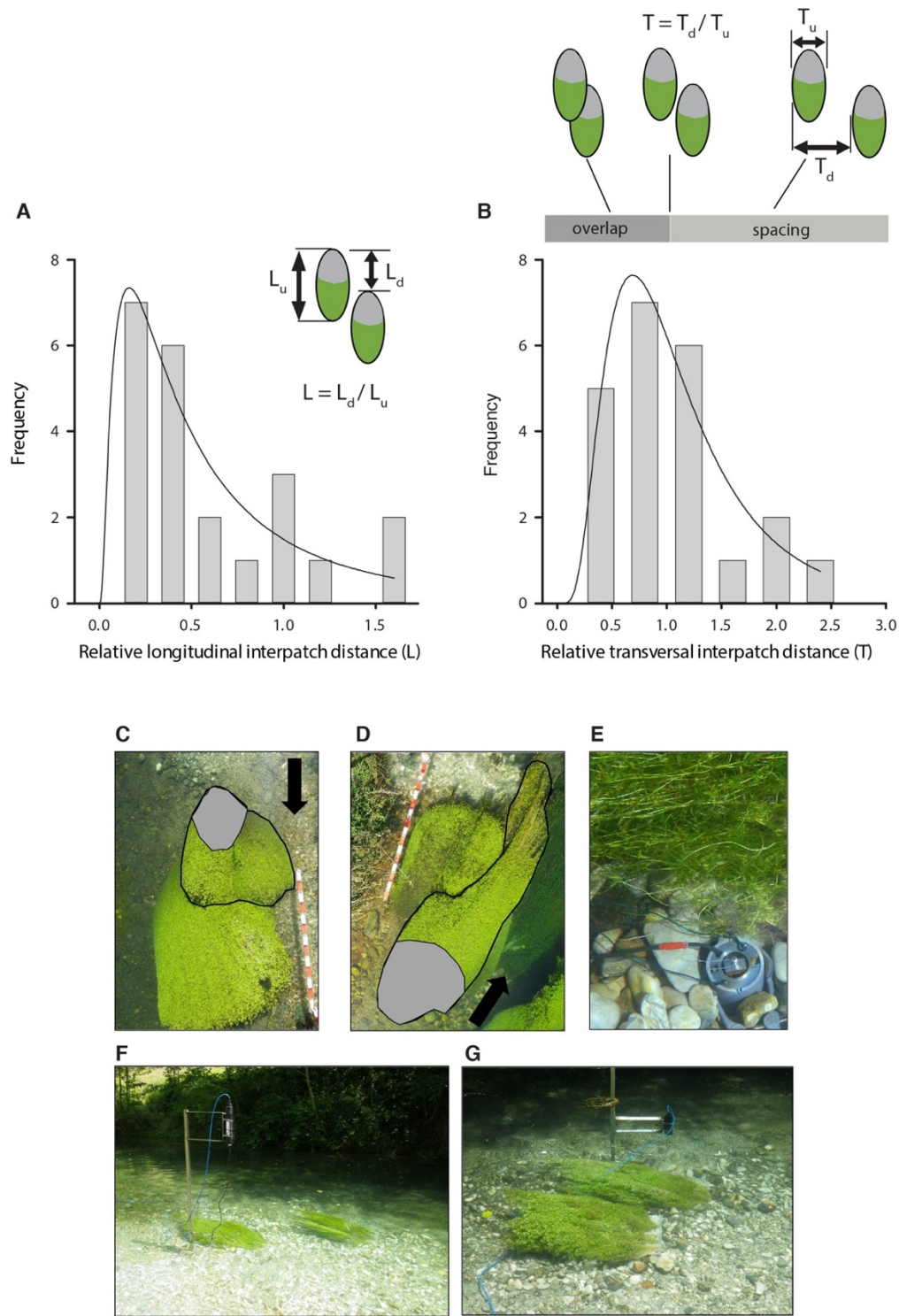|		Linear model			Quadratic model		
		Predictor variables					
		T * L	**T**	**L**	**T * L**	**T**	**L**
Relative $\overline{U}$ between patches	R^2	0.82	0.79	0.00	0.87	0.81	0.06
	p-value	0.01	0.0005	0.84	0.058	0.002	0.79
	AIC	-17.64	**-19.96**	-4.06	-16.99	-19.08	-2.67
Relative $\overline{U}$ upstream of patch "D"	R^2	0.40	0.24	0.05	0.71	0.33	0.28
	p-value	0.33	0.15	0.49	0.26	0.24	0.31
	AIC	-6.22	-7.71	-5.59	-9.37	-7.05	-6.28
Relative $\overline{U}$ next to patch "U"	R^2	0.41	0.22	0.00	0.90	0.25	0.69
	p-value	0.329	0.16	0.99	0.033	0.36	0.016
	AIC	-25.53	-26.77	-24.19	**-40.09**	-25.10	-33.95
Relative $\overline{U}$ next to patch "D"	R^2	0.33	0.31	0.00	0.38	0.31	0.085
	p-value	0.45	0.09	0.95	0.76	0.26	0.73
	AIC	-22.32	-26.05	-22.29	-19.15	-24.05	-21.18
TKE upstream of patch "D"	R^2	0.31	0.00	0.27	0.76	0.07	0.62
	p-value	0.48	0.99	0.11	0.18	0.77	0.03
	AIC	-80.09	-80.31	-83.53	-86.83	-79.04	**-87.99**

723

724

725 **Table 2** Changes in *Ranunculus* in-stream vegetation cover (%) and direction of growth of newly

726 occurring vegetation patches with respect to the nearest existing vegetation patch (°), based on field

727 observations in the Frome-Piddle catchment (UK), performed over three different time periods

728 covering the annual growth cycle. Observations were of the dominant species *Ranunculus*

729 *penicillatus* subsp. *pseudofluitans*.

		Dec. 2008	July 2009	Sept. 2009	Jan. 2010	July 2010	
Ranunculus cover (%)		13	22	7	22	30	
Angle to nearest vegetation patch (°)		Dec. 08 – July 09		Sept. 09 – Jan. 10		Jan. 10 – July 10	**Total**
Downstream	0 – 60	5		5		6	16
	60 – 120	0		3		1	4
	120 – 180	3		2		4	9
Upstream	180 – 240	1		0		5	6
	240 – 300	1		0		0	1
	300 – 360	1		0		1	2
Total		11		10		17	38
χ^2		9.20		12.80		10.88	24.34
d.f.		5		5		5	5
p- value		0.1		0.025		0.053	< 0.001

730

Figures

Figure 1 Frequency distribution of A) observed relative longitudinal inter-patch distance (distance

between upstream edges divided by upstream patch length) and B) relative transversal interpatch

735   distance (transversal gap between leftmost edges divided by upstream patch width) of neighbouring

736   patches of *Callitriche platycarpa*. The aerial pictures show macrophyte patch pairs (C, D) growing

737   in a staggered distribution, with overlapping canopies. The canopy of the upstream patch is outlined

738   in black. Grey areas indicate the extent of the rooted area. Arrows indicate main river flow

739   direction. E shows the force transducer employed in the field for drag measurements on

740   macrophytes. F and G illustrate the experimental setup in the field with the transplanted vegetation

741   patches and ADV for flow velocity measurements.
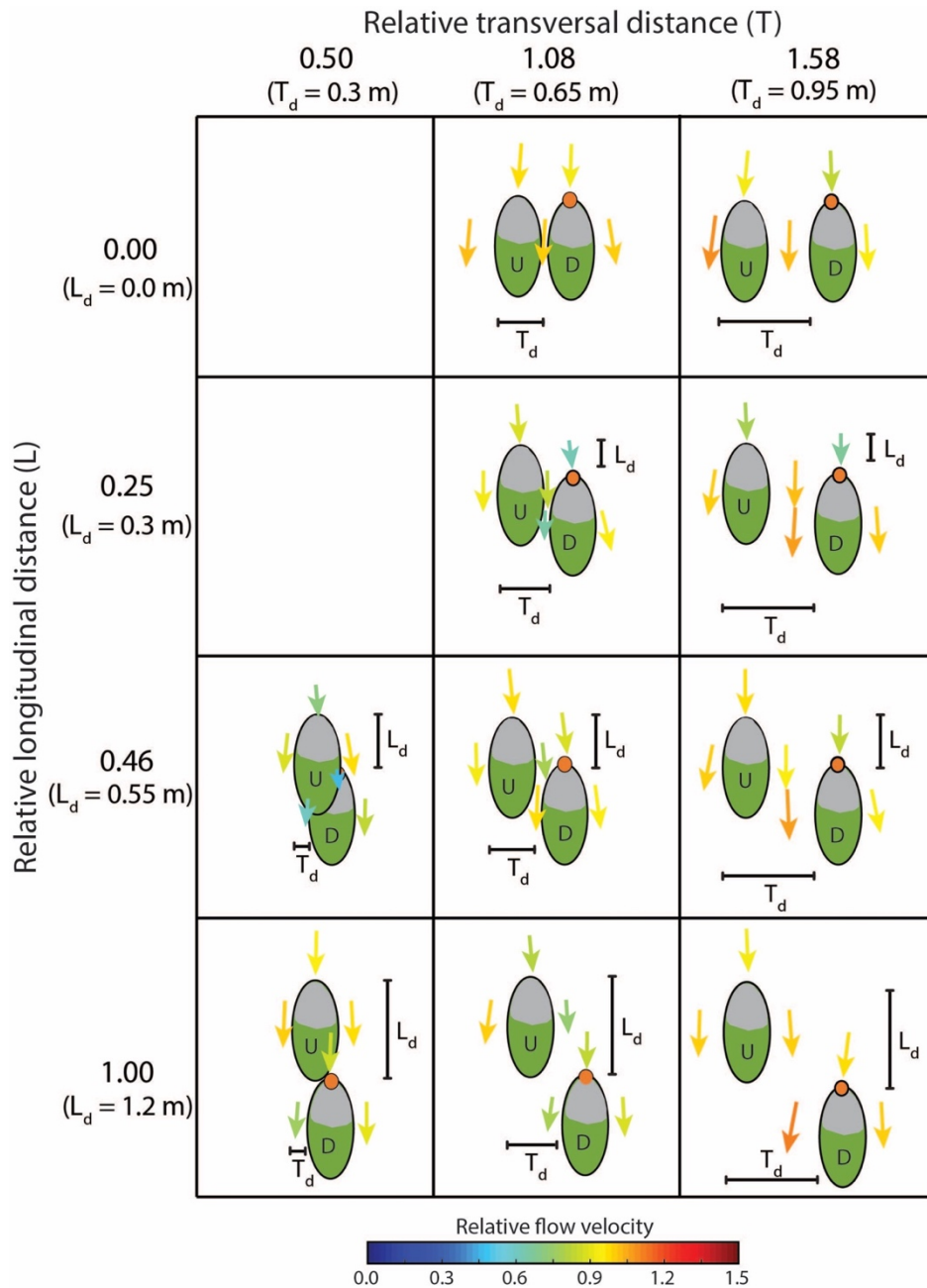
Figure 2 Overview of the ten patch configurations used in the field experiments, with indication of inter-patch distance in the longitudinal and transversal directions. L and T are relative distances; T_d and L_d are absolute distances (in m). Patch "U" was kept fixed, while patch "D" was moved downstream and/or laterally. Arrows indicate flow direction, and arrow size and colour indicate velocity magnitude relative to a measurement point located 0.5 m upstream of patch U. Grey areas indicate the extent of the rooted area. Orange dots are locations of drag measurements.

749
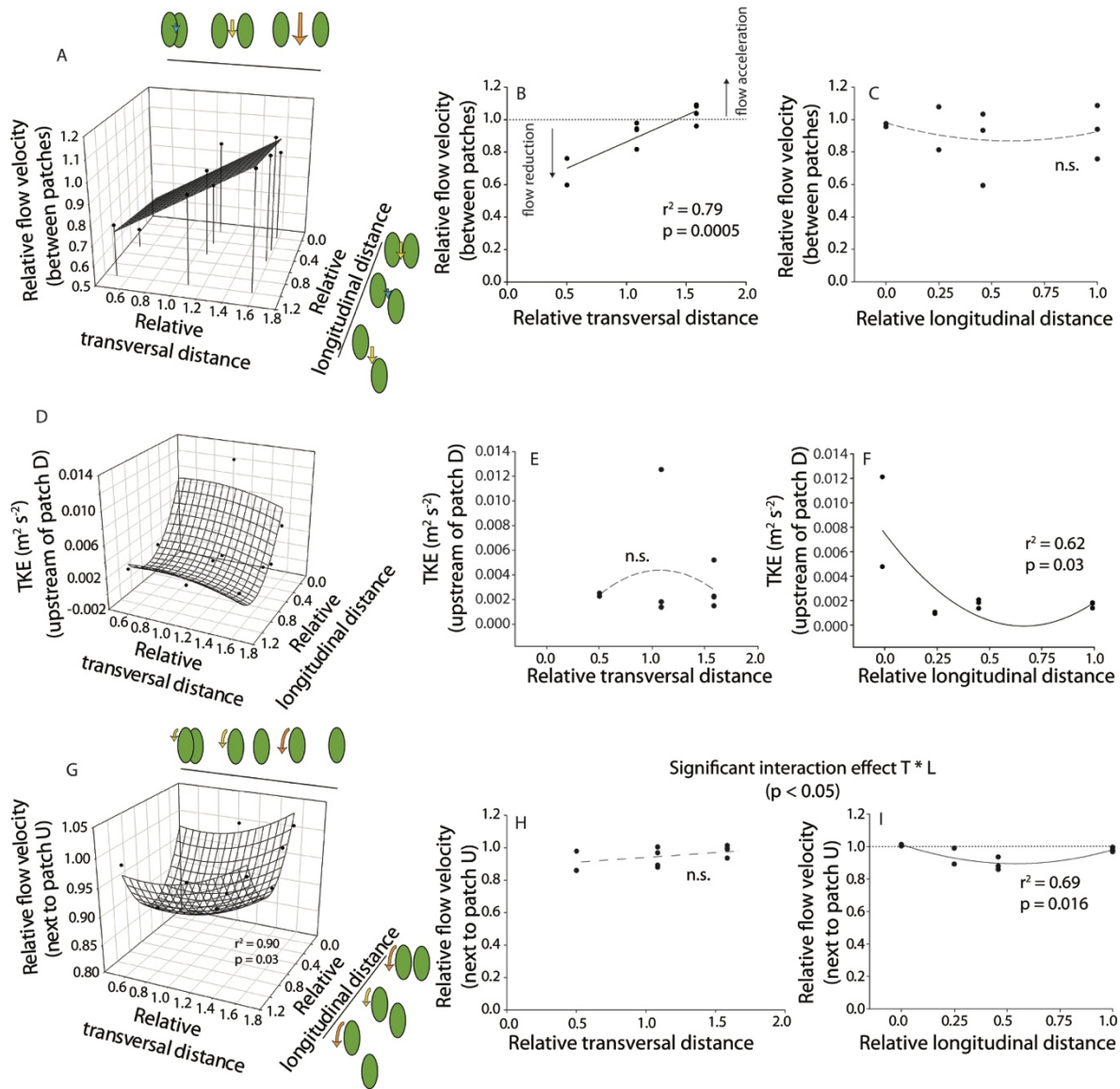
Figure 3 Relative flow velocity measurements (flow velocity relative to incoming flow) in between the patches (A, B, C) and on the side of patch U (G, H, I) for the ten configurations, showing the effects of increasing relative longitudinal and transversal distances. (D, E, F) Relationship between relative longitudinal and transversal distances and turbulent kinetic energy (TKE, m^2 s^{-2}) at the upstream edge of patch D. Green ovals are illustrations of the two neighbouring patches and their relative separation distances on the axes. Arrow size and colour indicate flow velocity magnitude, according to the colour scale in Figure 2.
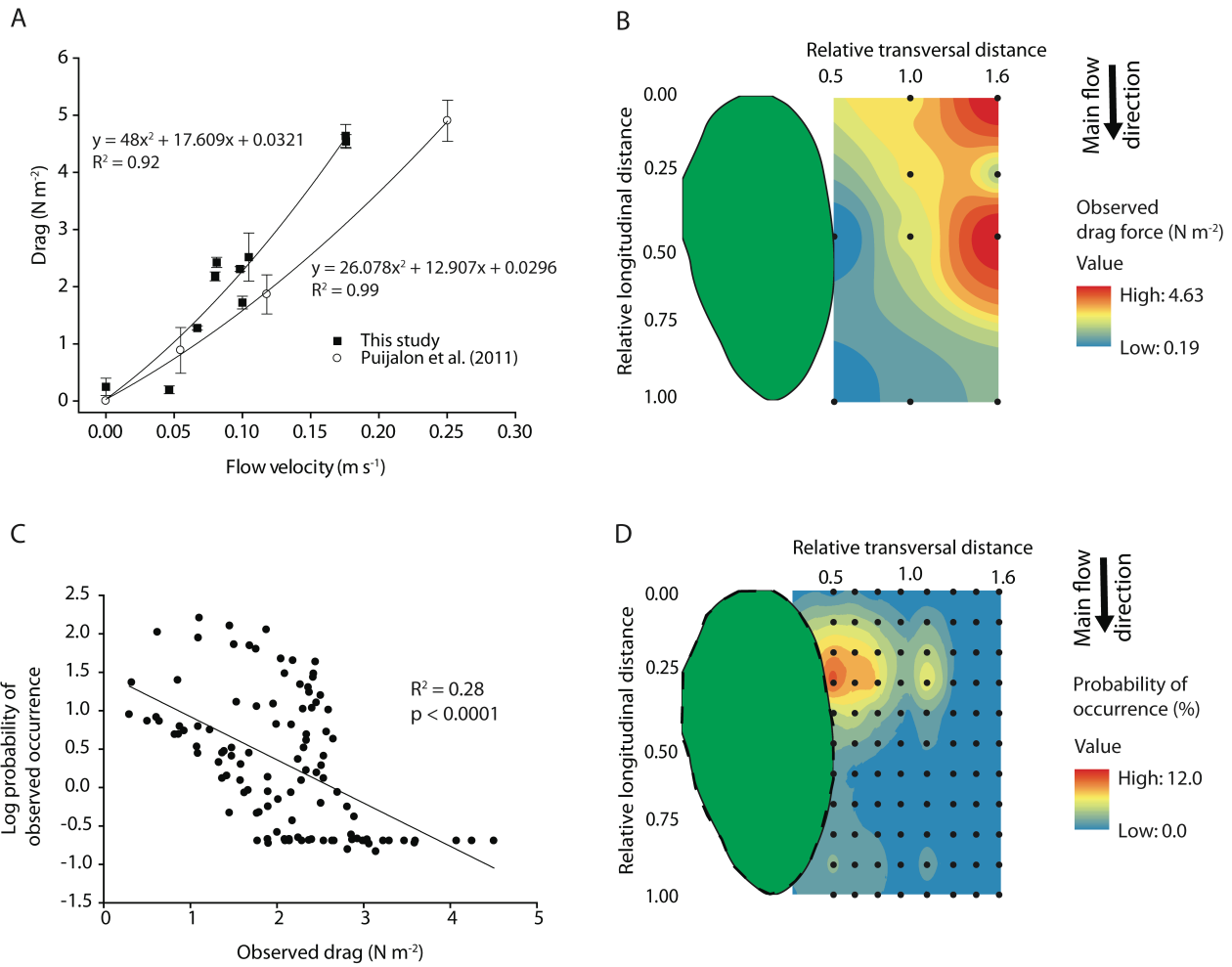
Figure 4 (A – B) Drag forces per unit surface area on single *C. platycarpa* individuals in different

positions around a vegetation patch in the field flume. In A, relationship between flow velocity and

drag force in the field (this study) and in a laboratory flume (Puijalon et al., 2011). In B, the drag

measurements (black dots, same points as in A) are plotted in an interpolated spatial grid around an

existing vegetation patch (in green). (C – D) Probability of observed patch occurrence around an

existing vegetation patch. In C, spatial regression between the experimental drag in a certain

position around a vegetation patch, and the probability of patch occurrence in the same position. In

D, map of probability of patch occurrence (%), based on the combination of the observed frequency

distributions of relative longitudinal and transversal distances in Figure 1. Black dots indicate the

767   grid of distance observations. Note that the vegetation patch (green oval with dashed line border)

768   provides an indication of the average size of an existing patch; the actual size observed in natural

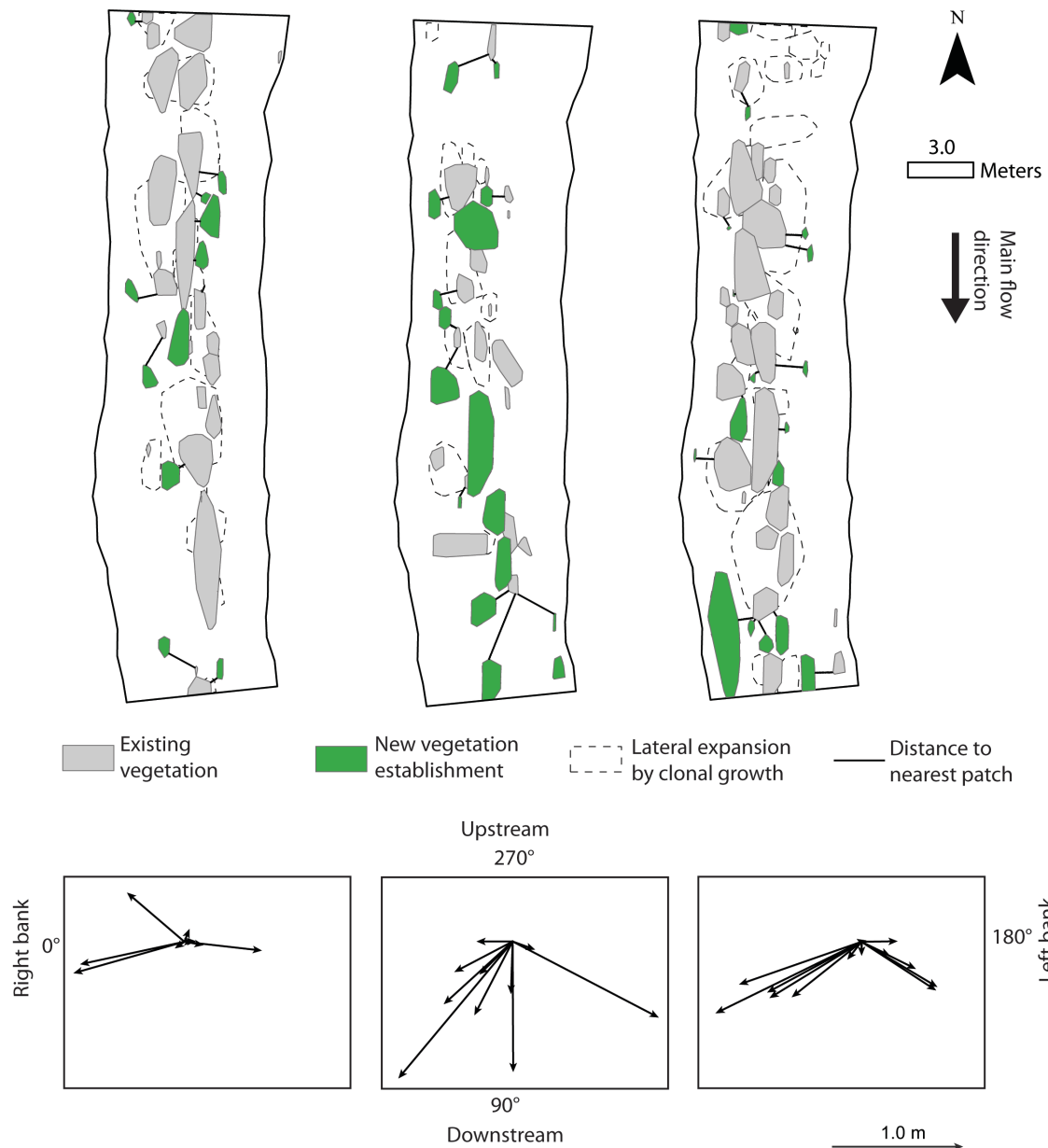769   neighbouring patches may vary.
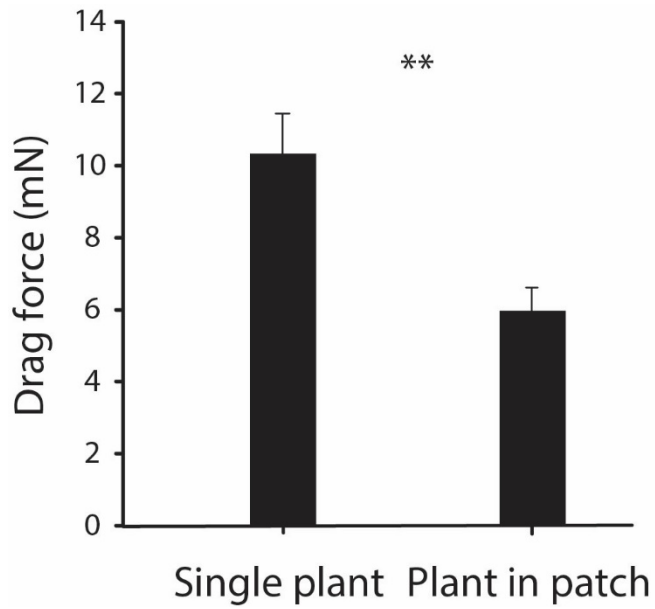
770

771 **Figure 5** Drag forces on a single plant vs. a plant located in a vegetation patch, averaged over the

772 ten vegetation configurations (paired t-test, $t_{19} = -2.2813$, p = 0.03). Error bars indicate standard

773 error.

774

Figure 6 *Top*: Planform representation of the distribution of in-stream macrophyte patches of

Ranunculus penicillatus subsp. *pseudofluitans*. In grey: existing vegetation patches at the start of

the survey period; dotted lines: lateral expansion of initial vegetation patches through clonal

growth; in green: new patches occurring at the end of the survey period. Black lines indicate the

shortest distance and direction of growth between the newly occurring vegetation and the nearest

781   existing patch. *Bottom*: distance and direction of growth (°) of new vegetation patches in each time

782   period over the stream bed.